The 5th Iranian International Conference on Microelectronics (IICM 2023)

October 25-26, 2023

2-D Axisymmetric Modeling of Circular PCB Coils and Solenoids in COMSOL Multiphysics

Farshad Gozalpour and Mohammad Yavari

Integrated Circuits Design Laboratory, Department of Electrical Engineering, Amirkabir University of Technology (Tehran Polytechnic), P.O. 15875-4413, Tehran 15914, Iran.

Emails: f.gozalpour@aut.ac.ir, myavari@aut.ac.ir

2023 5th Iranian International Conference on Microelectronics (IICM) | 979-8-3503-6019-6/23/$31.00 ©2023 IEEE | DOI: 10.1109/IICM60532.2023.10443210

***Abstract*—In this paper, a 2-dimentional (2-D) axisymmetric modeling is presented for biomedical circular printed circuit board (PCB) coils and solenoids in COMSOL Multiphysics. With this model, the number of required meshes in finite element method (FEM) based simulations is reduced, which speeds up the iterative design procedure of inductive links in biomedical implants. While having a good accuracy, the presented 2-D axisymmetric modeling reduces the extraction time of electromagnetic parameters of PCB coils and solenoids by about 90%, compared to 3-D modeling. In order to investigate the accuracy of presented 2-D modeling, we have fabricated a PCB coil and a solenoid with suitable geometries for implantation in body. The measurement results of electromagnetic parameters have a good agreement with the 2-D modeling based simulation results, and they verify each other. Finally, using the presented 2-D modeling, a comprehensive parametric simulation has been performed to study the behavior of coupling coefficient (*k*) and the maximum achievable *k* of PCB coils as a function of geometric parameters.**

Keywords—2-dimentional (2-D) axisymmetric modeling, circular PCB coil, solenoid, biomedical inductive link, electromagnetic parameters, COMSOL Multiphysics.

I. Introduction

Implantable medical devices (IMDs) with the main purpose of improving the body's organs with unusual performance have attracted special attention in recent years. They include cardiac pacemaker [1], brain-machine interface (BMI) [2], retinal prosthesis [3], cochlear implant [4], etc. The use of batteries to provide the power in IMDs requires periodic surgery due to the limited battery life-time. Meanwhile, wireless power transmission (WPT) provides a continuous and safe operation of IMDs without the need for wires passing through the skin that causes infection. As a result, the wireless operation of IMDs is essential to prevent infection and human comfortability. Inductive coupling is the oldest and predominant strategy of wireless transmission that can provide the power required by most biomedical systems (from a few milliwatts to several tens of milliwatts) with high reliability, safety, and efficiency. Circular printed circuit board (PCB) coils and solenoids play an important role in inductive links and their geometric parameters have a direct effect on the link characteristics.

In design of inductive links, in order to achieve the desired targets, usually an iterative procedure must be performed [5-12]. A general flow diagram of iterative design procedure in biomedical inductive links is illustrated in Fig. 1. Every

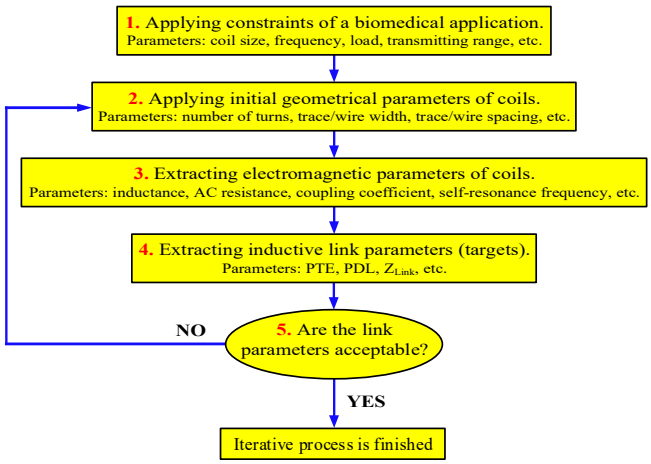

Fig. 1. A general flow diagram of iterative design procedure in biomedical inductive links.

biomedical application has its own design constraints and targets. The design constraints are mainly related to the working frequency, transmitting range, loading resistance, coil size, etc. First, using these constraints, initial values are applied for the geometric parameters of the coils such as number of turns, outer diameter, trace/wire width, trace/wire spacing, etc. Then, the electromagnetic parameters of the coils such as inductance, AC series resistance, parallel capacitance, coupling coefficient (*k*), etc., are derived and finally the parameters of the link performance such as power delivered to load (PDL) and power transmission efficiency (PTE) are obtained. If the achieved parameters are not acceptable in comparison with the design targets, this procedure should be repeated as far as the desired values are achieved. One of the factors that slows down this process is the finite element method (FEM) based simulations in extracting the electromagnetic parameters of the coils. Therefore, providing a two-dimensional (2-D) model for the coils can be an effective solution to this problem, considering that it converts 3-D volume of the geometry to 2-D domains and reduces the time required to solve the governing equations in defined geometry.

In this paper, using axisymmetric tools in COMSOL Multiphysics 5.5, a 2-D axisymmetric modeling for circular PCB coils and solenoids is proposed that can be utilized in most of previously published iterative design procedures of inductive links [5, 11, 12]. Since this model converts the 3-D volume of geometry to 2-D domains, FEM based simulations are performed more quickly, and as a result, the

required time in iterative procedure of extracting the electromagnetic parameters and the optimization of the link performance is significantly reduced. Finally, the proposed 2-D model has been applied and a comprehensive step-by-step parametric simulation is performed in order to study the effect of geometric variables of the coils such as outer diameter, number of turns, trace width and trace spacing on the behavior of coupling coefficient and the maximum achievable coupling between the PCB coils.

The rest of the paper is organized as follows. Section II presents the proposed 2-D axisymmetric modeling of circular PCB coils and solenoids. In section III, the 2-D modeling based simulation results and also the measurement results of the coil parameters are presented. Finally, conclusion is given in section IV.

II. 2-D Axisymmetric Modeling

Fig. 2(a) and Fig. 2(b) illustrate the top view of a circular PCB coil and a solenoid with their geometric parameters. In PCB coil, the parameters W, S, n, D_{out}, and D_{in} are trace width, trace spacing, number of turns, outer diameter, and inner diameter, respectively. In solenoid, the parameters n, p, l, D, and d are the number of turns, winding pitch, winding length, winding diameter, and wire diameter, respectively. The electrical model of PCB coil and solenoid is shown in Fig. 2(c), which includes the inductance L, AC series resistance R_S, AC parallel resistance R_P, and the parallel capacitance C_P. At low frequencies, the parallel resistance R_P can be ignored, and the self-resonance frequency and quality factor (Q) of PCB coil and solenoid are mainly determined by L, R_S, and C_P.

Fig. 3 shows the 2-D axisymmetric modeling of circular PCB coil and solenoid, where the rectangular and circular domains illustrate the cross-section area of conductor turns in PCB coil and solenoid, respectively. These domains are defined as a resistive-inductive-capacitive (RLC) coil group. They consider both in-plane and out-of-plane currents flowing in equilibrium condition that is required for 2-D modeling of the coils. The RLC coil group is a combination of magnetic model of a single-turn coil and a multi-terminal electrical model of in-plane current [13]. To define the arrangement for connection of domains, RLC group employs Bravais network that has two primary vectors **a** and **b** and provides two points $\mathbf{r}_1$ and $\mathbf{r}_2$: $\mathbf{r}_1$-$\mathbf{r}_2 = m_1\mathbf{a}+m_2\mathbf{b}$, where m_1 and m_2 are integer numbers. RLC coil group proposes n+1 electric potentials (V_0, V_1, ..., V_n), where V_0 is the reference voltage and n is the number of turns. The potential difference of the i-th turn is equal to:

$$V_i^d = V_i - V_{i-1} \tag{1}$$

where i = 1, ..., n. The potential difference for any turn gives the out-of-plane external current density ($\mathbf{J}_e$) as follows:

$$\mathbf{J}_e = \sigma \frac{V_i^d}{2\pi r}\mathbf{e}_\varphi \tag{2}$$

where $\mathbf{e}_\varphi$ is the out-of-plane unit vector, σ is the conductivity, and r is the vertical separation of the center of conductor cross-sections and the line r = 0. So, the out-of-plane current in i-th turn can be expressed by:

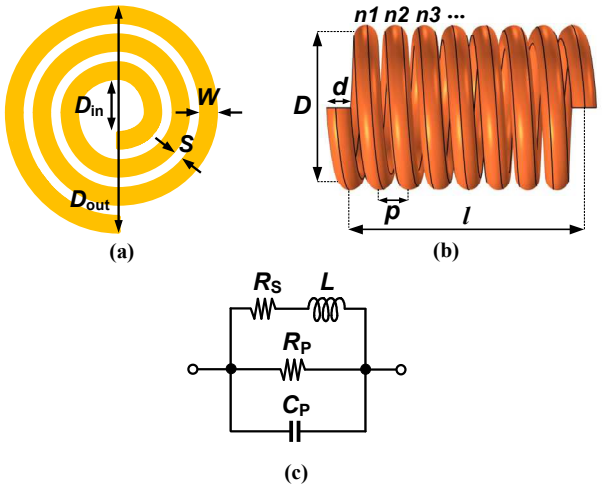

Fig. 2. (a) Circular PCB coil, (b) solenoid, (c) electrical model of PCB coil and solenoid.

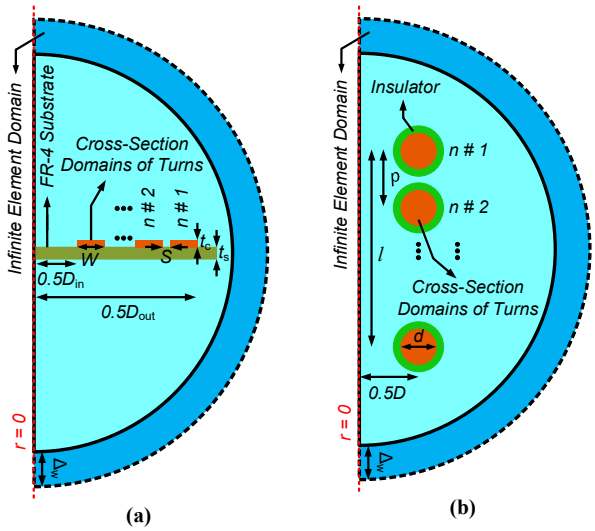

Fig. 3. 2-D axisymmetric modeling of (a) circular PCB coil and (b) solenoid.

$$I_i = \int_{\Omega_i} (\mathbf{J}.\mathbf{e}_\varphi) \tag{3}$$

Equilibrium condition between in-plane current and difference of out-of-plane currents in two neighboring turns implies [13]:

$$\begin{cases} I_i - \int_{\partial\Omega_i} (\mathbf{J}.\mathbf{n}) - I_{i+1} = 0 & i = 1,...,n-1 \\ I_n - \int_{\partial\Omega_n} (\mathbf{J}.\mathbf{n}) - I_{Coil} = 0 & i = n \end{cases} \tag{4}$$

where **n** is in-plane unit vector and I_{Coil} is the coil current. The electric potential is considered to have a constant value in cross section domain of turns, and therefore, this variable must be discarded in the mentioned domains by employing Ampere's law. The Ampere's law considers a $\mathbf{J}_e$ orthogonally to the domains, and also establishes a voltage limitation on the boundary of every cross-section domains of the turns. The magnetization, conduction and dielectric models needed for Ampere's law is considered as follows:

$$\mathbf{B} = \mu_0\mu_r\mathbf{H}, \quad \mathbf{J} = \sigma\mathbf{E}, \quad \mathbf{D} = \varepsilon_0\varepsilon_r\mathbf{E} \tag{5}$$

where **B**, **H**, **D**, and **E** are magnetic flux density, magnetic field, electric field intensity, and electric flux density, respectively. Also, μ_r, μ_0, ε_r, and ε_0 are relative permeability,

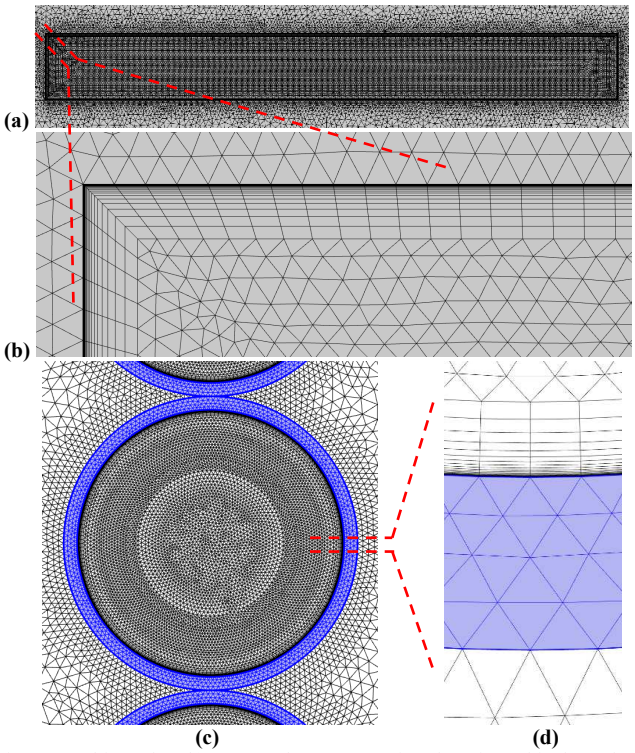

Fig. 4. Meshing of (a, b) rectangular cross-section domain and its boundary layer in PCB coil, (c, d) circular cross-section domain and its boundary layer in solenoid.

TABLE I GEOMETRIES OF THE FABRICATED PCB COIL AND SOLENOID.

Parameter	D_{out} [mm]	D_{in} [mm]	W [mm]	S [mm]	n
Circular PCB Coil	25.5	11.1	0.3	0.3	12
Parameter	D [mm]	d [mm]	p [mm]	l [mm]	n
Solenoid	3.22	0.2	0.22	9.46	43

permeability of free space, relative permittivity, and permittivity of free space, respectively.

The characterization of infinite domains is a common challenge in FEM simulations. In these simulations, artificial boundaries are usually used to limit the model to an area of interest. These boundaries must not influence the simulations inside the area of interest. In this paper, we have used infinite element domain (IED). The IED employs coordinate stretching in a virtual layer around the area of interest. The stretching function is defined as [14]:

$$f(\xi)=\frac{\xi}{\gamma-\xi}\Delta_p, \quad \gamma=\frac{\Delta_s+\Delta_p}{\Delta_s} \tag{6}$$

where ξ is the dimensionless coordinate ($0<\xi<1$), Δ_p is the pole distance, Δ_s is the scaled width of IED, and γ is a number larger than one. Δ_s and Δ_p are the primary parameters for stretching function. $f(\xi)$ returns a new stretched position, and therefore, the movement for stretching is defined as $\Delta\mathbf{x}=f_i(\xi)-\Delta_w\xi$, where Δ_w is the original width of infinite domain as shown in Fig. 3.

III. SIMULATION AND MEASUREMENT RESULTS

In order to investigate the accuracy of proposed 2-D axisymmetric modeling, we have fabricated PCB coil and solenoid with reported geometric parameters in Table I. The PCB coil is implemented on FR-4 PCB with substrate thickness (t_s) and copper thickness (t_c) of 1.6 mm and 0.035 mm, respectively. Also, the magnet copper wire is employed

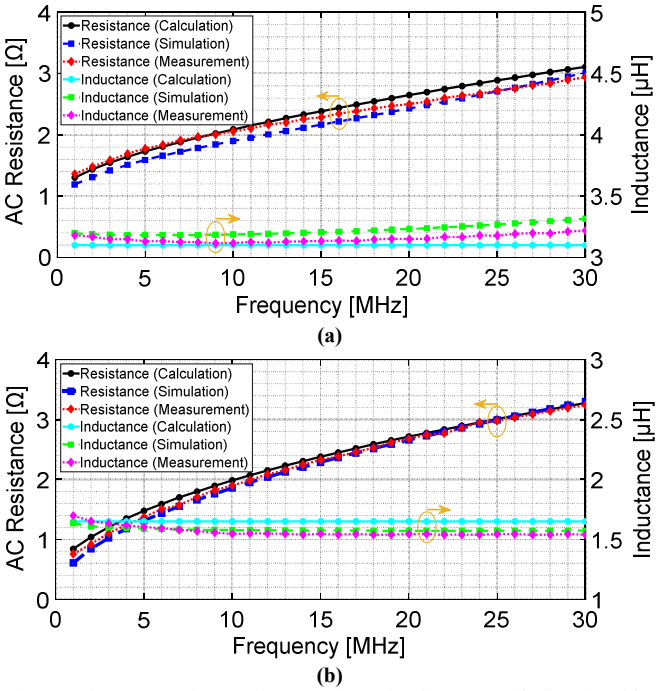

Fig. 5. Inductance and AC resistance of (a) circular PCB coil, (b) solenoid.

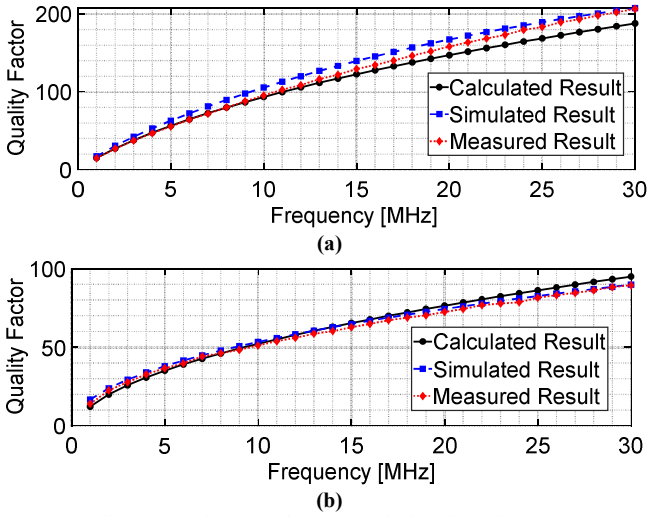

Fig. 6. Quality factor of (a) circular PCB coil, (b) solenoid.

for the solenoid. It should be noted that due to insulating layer of magnet wire in solenoid, p is slightly larger than d. In simulations, free triangular structure is used as the meshing of 2-D cross-section domains in geometry (Fig. 4). Also, boundary layer meshing is used for the boundaries of the cross-section domains of the turns. This is a meshing with compressed element distribution and is capable to estimate the skin effect on boundaries properly.

Fig. 5(a) and Fig. 5(b) depict the measured, simulated, and calculated inductance and AC series resistance in the range of 1 MHz to 30 MHz for circular PCB coil and solenoid, respectively. The measurement results have a good agreement with the 2-D modeling based simulation results, and they verify each other. It is worth mentioning that the measurement results of Fig. 5 have been obtained using the Wayne Kerr 6550P high frequency LCR meter with 1J1011 fixture connected to the front panel BNC sockets. Also, the calculations have been extracted by the conventional equations of PCB coils and solenoids [11, 15, 16].

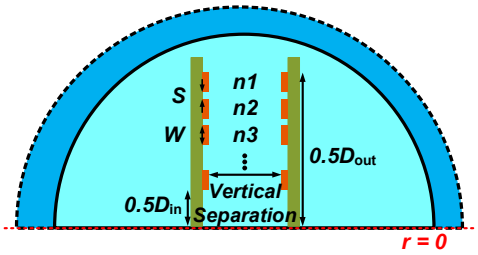

Fig. 7. 2-D simulation setup of coupling coefficient for PCB coils.

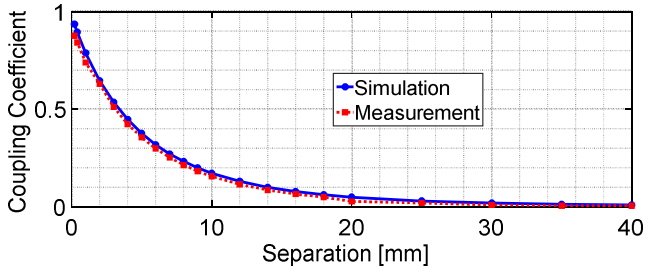

Fig. 8. Coupling coefficient of PCB coils with the geometries of Table I.

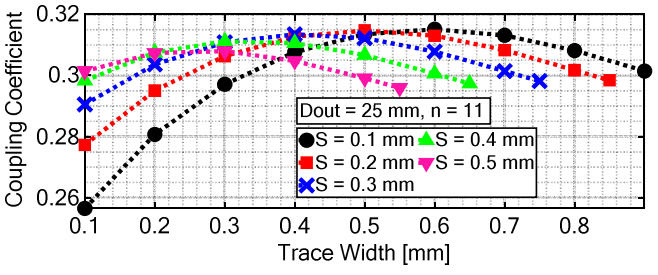

(a)

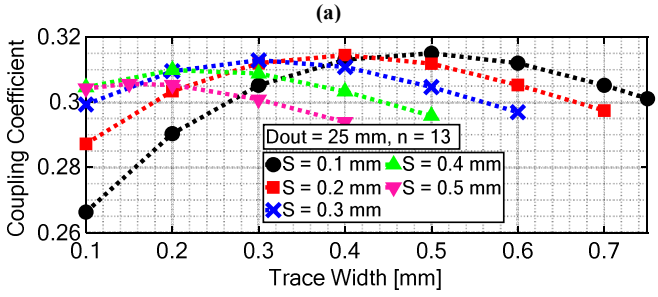

(b)

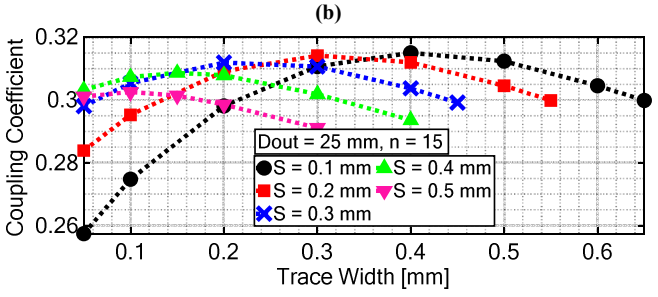

(c)

Fig. 9. Parametric sweep of coupling coefficient as a function of n, W and S: (a) n = 11, (b) n = 13, (c) n = 15.

Using the calculated, simulated, and measured inductance and AC series resistance, the calculated, simulated, and the measured quality factor (Q = ωL/R) of PCB coil and solenoid in the range of 1 MHz to 30 MHz are extracted and illustrated in Fig. 6(a) and Fig. 6(b), respectively. The measurement results have a good agreement with the 2-D modeling based simulation results, and they verify each other.

The simulation results of coupling coefficient (k) are based on the 2-D modeling of Fig. 7. Also, the measurement

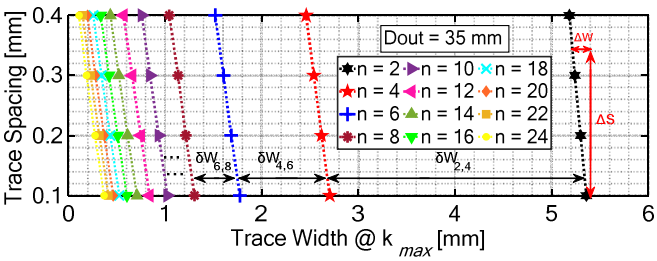

Fig. 10. Simulated S-$W_{k\text{-}max}$ lines for maximum coupling coefficient as a function of n (D_{out} = 35 mm).

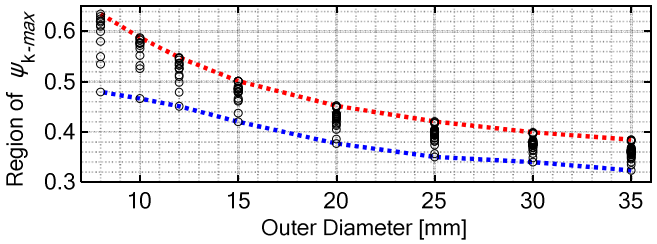

(a)

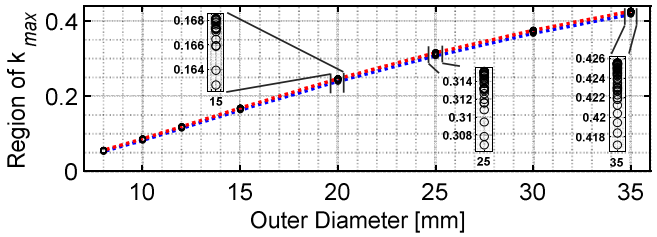

(b)

Fig. 11. (a) Region of $\Psi_{k\text{-}max}$ and (b) corresponding region of k_{max} for different D_{out}.

results are based on the measured voltage transfer function of inductive link with Rigol RSA3015N vector network analyzer. Fig. 8 illustrates the measured and simulated coupling coefficient between two circular PCB coils for the separation of 0.2 mm to 40 mm. The geometric parameters of both PCB coils are the same as Table I. According to Fig. 8, the measurement result has very good matching with simulation result and verifies the results of proposed 2-D model. It is worth mentioning that the simulation duration of coupling coefficient with 2-D model is only 25 sec, while it is equal to 350 sec for the conventional 3-D model. It can be seen that the simulation time has been drastically reduced by the proposed 2-D model.

In the next part of this section, a step-by-step parametric simulation is performed by 2-D axisymmetric modeling to study the behavior of maximum coupling coefficient of circular PCB coils as a function of geometric parameters such as D_{out}, n, W and S. In these simulations, the separation of PCB coils is kept as 6 mm. The simulation of Fig. 9 shows the k sweep for D_{out} = 25 mm and the different values of W and S. Also, the values of 11, 13, and 15 are selected for n in Fig. 9(a), Fig. 9(b), and Fig. 9(c), respectively. It can be observed that with increasing W, k is an increasing function of W to some extent, and then decreases. It is important to note that this increasing-decreasing behavior of k is independent of W, S and n. This behavior of k is also independent of D_{out}, which the corresponding results are reported in the next simulations.

In the next step, for the each S of 0.1 mm, 0.2 mm, 0.3 mm, and 0.4 mm, W is swept with much smaller steps to get the exact value of maximum k (k_{max}) and corresponding W

($W_{k\text{-}max}$). This simulation is performed for D_{out}=35 mm and different n, and the S-$W_{k\text{-}max}$ lines are shown in Fig. 10. Each S-$W_{k\text{-}max}$ lines corresponds to a specific n. $\delta W_{i,j}$ is the value of the shift between the lines $n = i$ and $n = j$. According to Fig. 10, $\delta W_{i,j}$ is approximately equal to:

$$\delta W_{i,j} = W_j = \frac{i}{j} W_i \tag{7}$$

where W_i and W_j are the $W_{k\text{-}max}$ for $n = i$ and $n = j$, respectively, and i and j can be any number of turns. This approximation is not limited to D_{out} = 35 mm and it holds for the all values of D_{out}. Also, the S-$W_{k\text{-}max}$ lines for a particular D_{out} have almost the same slopes ($\Delta S/\Delta W$).

In the final step, the parametric simulation of Fig. 10 is repeated for different values of D_{out} and the results are summarized in Fig. 11. $\Psi_{k\text{-}max}$ is the ratio of D_{in}/D_{out} where the k is maximized. This ratio is a function of coil geometric parameters such as W, S, n and D_{out}. Each of tiny circles in Fig. 11 corresponds to a specific D_{out}, W, S and n, where the k is maximized. The region of $\Psi_{k\text{-}max}$ as well as the corresponding region of k_{max} are shown in Fig. 11(a) and Fig. 11(b), respectively. It is observed that as D_{out} increases, the $\Psi_{k\text{-}max}$ decreases, meaning that k_{max} occurs at lower D_{in}/D_{out} ratios.

IV. Conclusion

In this paper, using axisymmetric tools in COMSOL Multiphysics, a 2-D axisymmetric modeling for biomedical circular PCB coils and solenoids is proposed that converts the 3-D volume of geometry to 2-D domains. Therefore, the FEM based simulations are performed more quickly, and as a result, the required time in iterative procedure of extracting the electromagnetic parameters and the optimization of the link performance is significantly reduced. As a comparison, the simulation of coupling coefficient with the proposed 2-D model and the conventional 3-D model is performed in 25 sec and 350 sec, respectively. The accuracy of 2-D based simulation results of electromagnetic parameters has been verified with the measurement results. Finally, the proposed 2-D model has been applied and a comprehensive step-by-step parametric simulation is performed in order to study the effect of geometric variables of the coils such as outer diameter, number of turns, trace width and trace spacing on the behavior of coupling coefficient and the maximum achievable coupling between the PCB coils.

References

[1] U. Anwar, O. A. Ajijola, K. Shivkumar, and D. Marković, "Towards a leadless wirelessly controlled intravenous cardiac pacemaker," *IEEE Trans Biomedical Engineering,* vol. 69, no. 10, pp. 3074-3086, Oct. 2022.

[2] J. P. Uehlin *et al.*, "A Single-Chip Bidirectional Neural Interface with High-Voltage Stimulation and Adaptive Artifact Cancellation in Standard CMOS," *IEEE J. Solid-State Circuits*, vol. 55, no. 7, pp. 1749-1761, Jul. 2020.

[3] A. Akinin *et al.*, "An optically addressed nanowire-based retinal prosthesis with wireless stimulation waveform control and charge telemetering," *IEEE J. Solid-State Circuits,* vol. 56, no. 11, pp. 3263-3273, Nov. 2021.

[4] F. Gozalpour and M. Yavari, "An Improved FSK-Modulated Class-E Power and Data Transmitter for Biomedical Implants," *AEU-Int. J. Electronics and Communications,* p. 154786, 2023.

[5] A. Ibrahim, and M. Kiani, "A figure-of-merit for design and optimization of inductive power transmission links for millimeter-sized biomedical implants," *IEEE Trans Biomedical Circuits and Systems,* vol. 10, no. 6, pp. 1100-1111, Dec. 2016.

[6] Y. Jia *et al.*, "A mm-sized free-floating wirelessly powered implantable optical stimulation device," *IEEE Trans Biomedical Circuits and Systems,* vol. 13, no. 4, pp. 608-618, Aug. 2019.

[7] U.-M. Jow, and M. Ghovanloo, "Design and optimization of printed spiral coils for efficient transcutaneous inductive power transmission," *IEEE Trans Biomedical Circuits and Systems,* vol. 1, no. 3, pp. 193-202, Sept. 2007.

[8] A. Khalifa *et al.*, "The microbead: A 0.009 mm 3 implantable wireless neural stimulator," *IEEE Trans Biomedical Circuits and Systems,* vol. 13, no. 5, pp. 971-985, Oct. 2019.

[9] M. Kiani, U.-M. Jow, and M. Ghovanloo, "Design and optimization of a 3-coil inductive link for efficient wireless power transmission," *IEEE Trans Biomedical Circuits and Systems,* vol. 5, no. 6, pp. 579-591, Dec. 2011.

[10] A. K. RamRakhyani, S. Mirabbasi, and M. Chiao, "Design and optimization of resonance-based efficient wireless power delivery systems for biomedical implants," *IEEE Trans Biomedical Circuits and Systems,* vol. 5, no. 1, pp. 48-63, Feb. 2010.

[11] M. Schormans, V. Valente, and A. Demosthenous, "Practical inductive link design for biomedical wireless power transfer: A tutorial," *IEEE Trans Biomedical Circuits and Systems,* vol. 12, no. 5, pp. 1112-1130, Oct. 2018.

[12] M. Kiani and M. Ghovanloo, "A figure-of-merit for designing high-performance inductive power transmission links," *IEEE Trans Industrial Electronics,* vol. 60, no. 11, pp. 5292-5305, Nov. 2013.

[13] C. Multiphysics, "AC/DC Module User's Guide for COMSOL," *Stockholm, Sweden: COMOSOL AB*, 2013.

[14] https://doc.comsol.com/5.5/doc/com.comsol.help.comsol/comsol_ref_definitions.12.115.html

[15] D. W. Knight, "An introduction to the art of solenoid inductance calculation with emphasis on radio-frequency applications," Feb. 2016, [Online]. Available: http://g3ynh.info/zdocs/magnetics/part_1.html

[16] D. W. Knight, "Selonoid Impedance and Q" Jan. 2016, [Online]. Available: http://g3ynh.info/zdocs/magnetics/solenz.html